

Modes of seafloor generation at a melt-poor ultraslow-spreading ridge

Mathilde Cannat Equipe de Géosciences Marines, CNRS-UMR 7154, Institut de Physique du Globe, 4 place Jussieu, 75252 Paris cedex 05, France

Daniel Sauter
Véronique Mendel Institut de Physique du Globe, 5 rue Descartes, 67084 Strasbourg cedex, France

Etienne Ruellan Géosciences Azur, CNRS-UMR 6526, 250 rue A. Einstein, Sophia Antipolis, 06560 Valbonne, France

Kyoko Okino Ocean Research Institute, University of Tokyo, 1-15-1 Minamidai, Nakano, Tokyo 164-8639, Japan

Javier Escartin
Violaine Combier Equipe de Géosciences Marines, CNRS-UMR 7154, Institut de Physique du Globe, 4 place Jussieu, 75252 Paris cedex 05, France

Mohamad Baala Institut de Physique du Globe, 5 rue Descartes, 67084 Strasbourg cedex, France

ABSTRACT

We report on extensive off-axis bathymetry, gravity, and magnetic data that provide a 26-m.y.-long record of axial tectonic and magmatic processes over a 660-km-long and melt-poor portion of the ultraslow Southwest Indian Ridge. We describe a new type of seafloor (the smooth seafloor) that forms at minimal ridge melt supply, with little or no axial volcanism. We propose possible mechanisms leading to this avolcanic or nearly avolcanic mode of spreading, in contradiction with the traditional view of mid-ocean ridges as primarily volcanic systems. We also show evidence for large-offset asymmetric normal faults and detachments at the ridge axis, with asymmetry persisting in some cases for tens of millions of years.

Keywords: mid-ocean ridges, avolcanic, ultraslow spreading, tectonic asymmetry.

INTRODUCTION

Ultraslow accretion (<20 mm/yr) occurs along 20% of the Earth's mid-ocean ridge system, and exposes large expanses of mantle-derived peridotites in the seafloor, thus raising questions about the nature of the oceanic crust in these environments. Whole sections of the ultraslow Southwest Indian Ridge, and of Gakkel Ridge in the Arctic Ocean, have this characteristic, and have been inferred to reflect amagmatic seafloor spreading (Dick et al., 2003).

Our new bathymetry, gravity, and magnetic data for the eastern Southwest Indian Ridge are the most extensive available for an ultraslow ridge, covering nearly twice the area of Iceland and extending as much as 250 km off axis on both plates (crustal ages to 28 Ma; Fig. 1). The eastern Southwest Indian Ridge and the sparsely magmatic zone of Gakkel Ridge are among the deepest ridges on Earth, and have an average crustal thickness of 3–4 km (Cannat et al., 2003; Muller et al., 1999; Jokat et al., 2003; Michael et al., 2003; Meyzen et al., 2003). Regional ridge depth and crustal thickness can be used to infer variations in melt supply to mid-ocean ridges (Klein and Langmuir, 1987). Our study area and the deepest part of Gakkel Ridge are therefore inferred to represent a melt-poor end member for the ridge system worldwide. Our data provide the first opportunity to study the time and space evolution of spreading processes in this end-member spreading context.

SPREADING RATE AND PLATE BOUNDARY GEOMETRY

Data (picks) for magnetic anomalies A1–A8 (0.78–26.5 Ma; the magnetic time scale of Cande and Kent [1995] is used throughout) indicate a mean finite spreading rate of ~14 km/m.y. between A6 and A1, with <10% asymmetry between the two flanks. Faster rates of ~16 km/m.y., then 30 km/m.y., are inferred for the crust formed respectively between anomaly 6 and 6C, and prior to anomaly 6C (24.12 Ma), consistent with earlier studies immediately to the west of our survey area (Patriat and Segoufin, 1988).

Magnetic anomalies also show that the plate boundary geometry in our study area has been stable over at least the past 26 m.y. (magnetic anomaly A8 to present; Fig. 1B). Southwest Indian Ridge finite opening poles published for this time interval (Lemaux et al., 2002; Patriat and Segoufin, 1988) fit our picks and correspond to spreading directions between 175° and 190°. Present-day ridge obliquity was therefore maintained over at least the past 26 m.y., with the same contrast between a region of oblique spreading in the west, and a region of near-orthogonal spreading in the east (Fig. 1).

THREE TYPES OF SEAFLOOR MORPHOLOGY

Details of basement morphology are visible even in the oldest parts of our bathymetric map and allow us to identify three distinct

types of seafloor, only one of which shows evidence for a volcanic upper crustal layer.

1. Volcanic seafloor displays numerous volcanic cones and occasional flat-topped volcanoes. Tight, spreading-perpendicular to slightly oblique fault scarps extend 2–20 km along axis; heaves range from <50 m to >500 m. These scarps face the axis and face away from it, bounding horsts and grabens in a similar manner to the abyssal hills described at faster spreading seafloor (Macdonald et al., 1996). The volcanic terrain is the most abundant, representing ~59% of the total mapped surface (Fig. 2E).

2. Smooth seafloor occurs in the form of broad ridges, with a smooth, rounded topography, no volcanic cones, and no scarps. The ridges are 15–30 km long, 500–2000 m high, and follow the local ridge trend at the time they were formed (Fig. 2). Some are symmetrical (Fig. 2C); others have steeper outward-facing than inward-facing slopes (Fig. 2D). Smooth seafloor represents 37% of the total mapped area. All dredges so far in smooth seafloor parts (Fig. 2E) have sampled serpentinized peridotites, with or without gabbros and basalts (Seyler et al., 2003). Exposure of mantle-derived rocks thus appears to be the rule rather than the exception in these terrains. The absence of volcanic edifices is confirmed by available deep-tow sonar data (Sauter et al., 2004). This smooth seafloor morphology is described here for the first time. It is, however, probably also present at amagmatic accretionary ridge segments that have been described in other regions of the Southwest Indian Ridge, and at Gakkel Ridge (Dick et al., 2003; Michael et al., 2003).

3. Corrugated seafloor occurs in the form of domes, or subhorizontal areas, free of volcanic cones but showing spreading-parallel undulations of the seafloor (Figs. 2A, 2B, 2D). These undulations are <1 km wide, 30–100 m high, and extend as much as 20 km in the direction of spreading. Individual undulated or corrugated surfaces extend 4–73 km in the along-axis direction, and 4–30 km in the

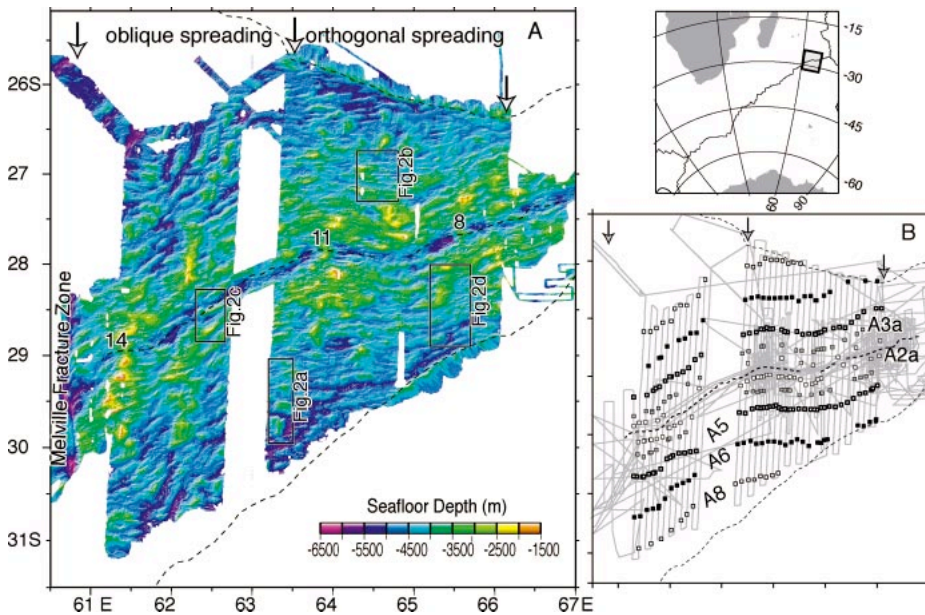


Figure 1. Eastern Southwest Indian Ridge and surrounding seafloor. Seafloor depth (A) and picks for magnetic anomalies (B). Data are from cruise 135 of RV *Marion Dufresne* and earlier cruises (see footnote 1). Dashed lines are traces of Rodriguez Triple Junction and present-day ridge axis. Insets a–d in A show location of detailed maps in Figure 2. Numbers 8, 11, and 14 refer to ridge segment numbers for three large present-day volcanic centers (Cannat et al., 1999). Spreading is oblique in west (33° angle between spreading direction and ridge-perpendicular direction), and nearly orthogonal in east.

spreading direction. Similar corrugated surfaces were first discovered in the Atlantic (Cann et al., 1997). Dredges there have yielded fault rocks (Escartin et al., 2003), and the domal topography has been reproduced in numerical

models by rotations of the footwall of large-offset normal faults (Lavier et al., 1999). Corrugated surfaces are therefore thought to expose the inactive footwall of large-offset, axial valley–bounding normal faults, also called de-

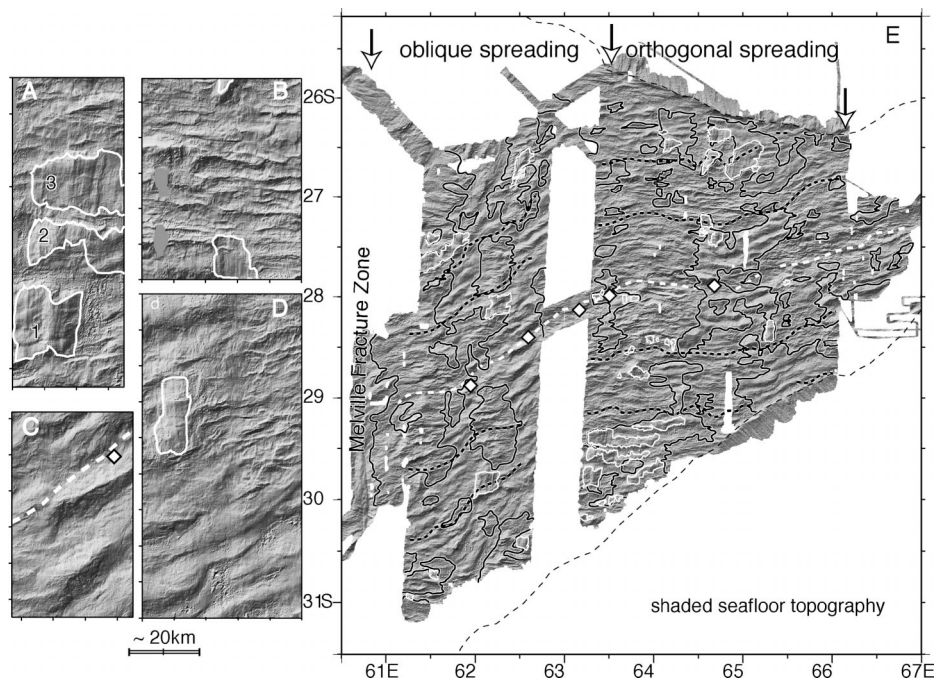


Figure 2. Seafloor slope illuminated from 330°. A–D: Detail maps (located in Fig. 1A). Open diamonds in C and E—dredged mantle-derived peridotites, with or without gabbros and basalt (Seyler et al., 2003). Thick black dashed lines in E are 10 and 20 m.y. isochrones drawn from pickings of magnetic anomalies 5 and 6. Black contours in E are limits of volcanic terrains. White contours are corrugated surfaces; 39 have been identified, only one of which was known previous to this study (Searle et al., 2003).

tachment faults (Cann et al., 1997; Tucholke et al., 1998). In our study area, they represent ~4% of the total mapped surface.

GRAVITY ANOMALIES, CRUSTAL THICKNESS, AND MELT SUPPLY

Gravity anomalies reflect the density structure of the crust and upper mantle. They can be used to model variations in crustal thickness (Kuo and Forsyth, 1989), if lateral density variations within these two horizons are small. There may, however, be significant lateral density variations within the crust, particularly where mantle-derived rocks are exposed in the seafloor. We thus base our analysis of gravity data primarily on residual mantle Bouguer anomalies (RMBA; Fig. 3A). RMBA lows correspond to thicker constant density model crust (to 8 km thick; Data Repository Fig. DR1¹), or to lighter material, and RMBA highs correspond to thinner constant density model crust (as thick as 0.5 km), or to denser crustal or upper mantle material.

Smooth seafloor and most corrugated terrains correspond to high RMBA values (Fig. 3A). This is consistent with a lower magma input, all the more for the smooth seafloor terrain, because part of the crust there is made of exhumed mantle-derived peridotites. Corrugated surfaces also occur in areas of moderate RMBA (Fig. 3A), from which we infer that they also form when the ridge magma supply is somewhat higher.

RMBA lows in Figure 3A show a striking pattern of bull’s-eyes. On axis, these bull’s-eyes correspond to the three large active volcanic centers (ridge segments 8, 11, and 14 in Fig. 1). From this, we infer that off-axis gravity low bull’s-eyes correspond to past events of similarly focused ridge magmatism (Cannat et al., 2003). Volcanic terrains extend out of the gravity low bull’s-eyes (Fig. 3A) into areas of higher RMBA values. Based on observations at the present-day ridge axis (Sauter et al., 2004), we propose that these higher RMBA volcanic areas form by lateral propagation of dikes away from the bull’s-eyes volcanic centers.

Low RMBA bull’s-eyes between 63°15’E and 64°30’E occur only in the northern, African plate (Fig. 3A), indicating that past volcanic centers there have been rafted preferentially to the north. This pattern has no equivalent in other sets of mid-ocean gravity data. Our preferred interpretation is that north-facing, large-offset axial normal faults have

¹GSA Data Repository item 2006113, additional references, details on processing of gravity data, plate rotation parameters used to produce Fig. 4, and histograms of RMBA values in the oblique and orthogonal-spreading regions, is available online at www.geosociety.org/pubs/ft2006.htm, or on request from editing@geosociety.org or Documents Secretary, GSA, P.O. Box 9140, Boulder, CO 80301, USA.

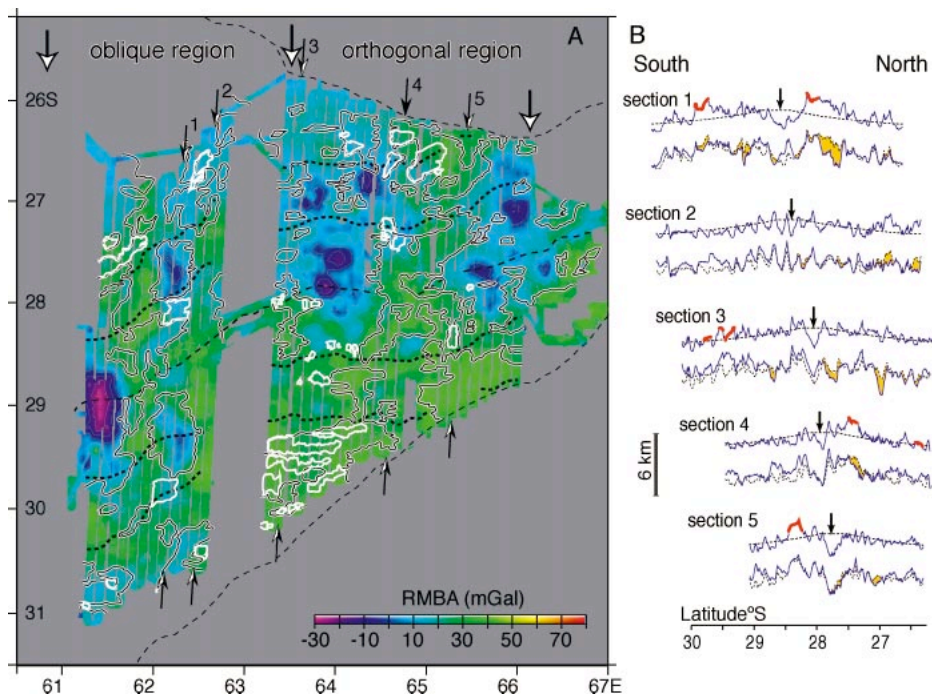


Figure 3. Residual mantle Bouguer gravity anomaly (RMBA, A), and crustal thickness modeled from gravity for five cross-axis sections (B). RMBA was calculated from ship free-air gravity by subtracting effects of topography and constant density, 3.4-km-thick reference crust, and of upper mantle cooling with age (see footnote 1). Numbered black arrows in A show location of sections in B. Blue lines: seafloor topography and base of gravity-derived model crust (Fig. DR1; see footnote 1); dashed lines: predicted subsidence; dotted lines: base of constant thickness reference crust. Yellow: modeled crust is thicker than reference crust. Red: corrugated surfaces; arrows: location of ridge axis.

prevailed in this 120-km-long portion of the ridge since the initiation of Southwest Indian Ridge spreading ~28 m.y. ago. This led to the preferred accretion of lower density, crustal, hanging-wall material to the northern plate, and to the formation of a large group of corrugated surfaces (prior to magnetic anomaly 6; Fig. 3A) in the southern plate.

THREE PRINCIPAL MODES OF MELT-POOR ULTRASLOW SPREADING

The sections in Figure 3B recall numerical models of oceanic lithosphere created at ridges with a thick axial lithosphere and large offset axial normal faults (Buck et al., 2005). These faults modify the axial crustal structure and locally produce strong asymmetry between the two ridge flanks.

Volcanic seafloor is most commonly accreted to both plates; this configuration accounts for 40% of the seafloor in our study area (Figs. 4 and 5A). Volcanic seafloor is less commonly accreted on one plate, whereas corrugated (Fig. 5B) or smooth (Fig. 5C) seafloor forms in conjugate crust.

In Figure 5A, successive large offset normal faults are inferred to develop preferentially in one ridge flank, producing a long-lasting asymmetry of crustal thickness and gravity signature between the two plates (as observed in the 63°15'E–64°30'E region; Fig. 3A). Suc-

cessive principal axial faults in Figure 5A can also face alternatively north and south, producing an overall symmetrical crustal thickness (and gravity) pattern.

Corrugated seafloor in Figure 5B is inferred to form in the footwall of a detachment fault, with dikes and lava in the conjugate, hanging-wall plate. This configuration accounts for only 7% of the seafloor accreted in our study area (Fig. 4). The corrugated surface mode thus appears to correspond to a narrow window of magmatic and/or tectonic conditions, as proposed on the basis of numerical models of axial faulting (Buck et al., 2005). Some corrugated surfaces have a large extension along axis, others are very narrow. Such narrow surfaces likely represent the exposed portion of wider detachment faults buried beneath entrained blocks of hanging-wall volcanics (Reston and Ranero, 2005).

Smooth seafloor is either accreted to both plates (23% of total mapped area; Fig. 4), or faces volcanic seafloor in conjugate crust (this second configuration forms 28% of total mapped area). We propose that smooth seafloor forms by frequent shifts in the polarity of axial valley–bounding normal faults and shear zones, leading to fault capture, and to an essentially symmetrical overall tectonic pattern (Fig. 5C; Cannat et al., 1997). The ridge-parallel trend of the observed horst and

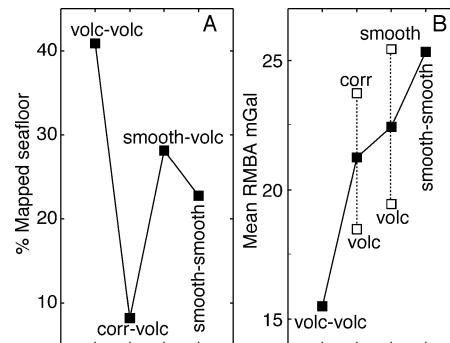


Figure 4. Plate rotation parameters (Table DR1; see footnote 1) are used to compare seafloor morphology in lithosphere inferred to have formed simultaneously on each side of axial valley. Four types of conjugate seafloor morphologies (volcanic-volcanic, corrugated-volcanic, smooth-volcanic, and smooth-smooth) represent 98% of mapped surface and are plotted in order of increasing surface (A), and mean residual mantle Bouguer gravity anomaly (RMBA, B). Within corrugated-volcanic and smooth-volcanic pairs, conjugate volcanic seafloor systematically has lower mean RMBA (or thicker crust). Corrugated-smooth conjugates represent 2% of mapped surface, which we consider to be within margin of error of our reconstructions (see footnote 1).

graben morphology, even in oblique-spreading regions, suggests that failure is localized by the axis of lithospheric necking at the base of the plate (Dick et al., 2003). Smooth seafloor occasionally bears faint corrugations, suggesting that, in favorable conditions (e.g., higher melt supply), axial valley–bounding faults in Figure 5C evolve into corrugated detachments (Fig. 5B).

EFFECT OF RIDGE OBLIQUITY

The smooth terrain is more abundant (50% of mapped area) and forms flow line–parallel bands in the oblique spreading region to the west of our study area. It is less abundant (28% of mapped area) and forms irregular expanses in the orthogonal spreading region to the east (Fig. 2E). Average RMBA values are similar in the two regions (Fig. DR3; see footnote 1), suggesting similar overall melt supply, and contradicting the hypothesis of a strong effect of spreading obliquity on melt supply at ultraslow ridges (Dick et al., 2003). Instead, we propose that, for a given melt supply, ridge obliquity favors avolcanic spreading by limiting the lateral propagation of dikes from nearby volcanic centers.

CONCLUDING REMARKS

Of the three spreading modes sketched in Figure 5, two (volcanic-volcanic and corrugated-volcanic) also develop at the faster spreading Mid-Atlantic Ridge, and at more magmatically robust regions of ultraslow ridges (Hosford et al., 2003; Mendel et al., 2003). By contrast, the smooth terrain identified for

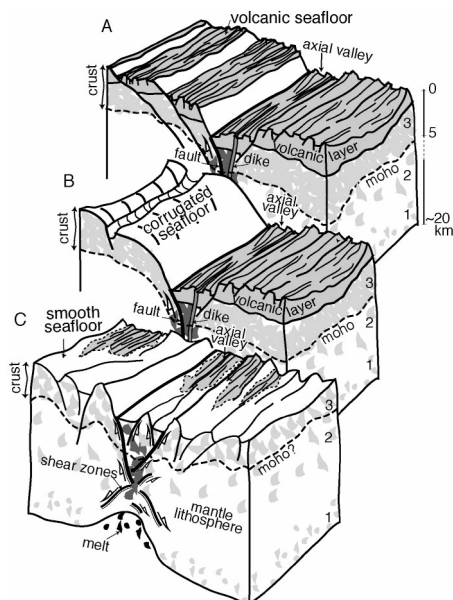


Figure 5. Lithosphere-scale sketches of axial region for three proposed modes of melt-poor ultraslow spreading, shown in order of inferred decreasing melt supply. Modes A (volcanic-volcanic) and B (corrugated-volcanic) also develop at faster spreading Mid-Atlantic Ridge, and in more magmatically robust regions of ultraslow ridges. Mode C (smooth-smooth or smooth-volcanic), with little to no axial volcanism, appears specific to melt-poor ultraslow ridges. Horizontal dimensions are ~80 km across axis, and ~40 km along axis. Melt concentrations are shown in black (in asthenosphere), or dark gray (in lithosphere). Crystallized magmatic rocks are shown in lighter shade of gray. Abundance of magmatic rocks at different levels of crust and mantle lithosphere (1, 2, and 3) is expected to vary as a function both of how much melt crystallized at which depth, and of how much of crystallized material was then tectonically transported to higher levels (Cannat, 1996).

the first time in our study area appears specific to melt-poor, ultraslow seafloor, and forms at portions of the ridge where volcanism is scarce to absent. This avolcanic, or nearly avolcanic, mode of seafloor spreading may be analogous to processes at the ocean-continent transition of continental margins (Whitmarsh et al., 2001), and appears to have created nearly half of the oceanic crust in our study area. This contradicts the traditional view of all mid-ocean ridges as primarily volcanic systems. Lack of volcanism, however, does not mean that smooth terrains are strictly amagmatic and expose only unroofed mantle-derived ultramafic rocks. A thick axial lithosphere could favor melt crystallization as intrusions at different levels of the crust and upper mantle (Cannat, 1996), as sketched in Figure 5. In fact, most dredges in smooth terrains also include some basalts and/or gabbros (Seyler et al., 2003).

Another remarkable characteristic is the

persistent asymmetry of the lithosphere's gravity signature in the region 63°15'E–64°30'E (Fig. 3A), suggesting very long lasting (~28 m.y.) tectonic asymmetry at this 120-km-long portion of the ridge axis. By contrast, in other regions of our study area, axial tectonic asymmetry as inferred from the distribution of corrugated surfaces and from gravity anomalies appears to have flipped polarity, over periods of a few million years only. Identifying the factors that led either to long-lasting axial tectonic asymmetry, or to frequent flips in fault polarity, is an important goal for future studies.

ACKNOWLEDGMENTS

We thank Captain J.P. Hedrich and his crew, and the Institut Paul Emile Victor (IPEV) team of marine engineers led by A. Jaouen, for their work during cruise 135 of RV *Marion Dufresne* in October 2003. Funding was provided by IPEV and the Centre National de la Recherche Scientifique–Institut des Sciences de l'Univers (Dynamique et Evolution de la Terre Interne). This is Institut de Physique du Globe de Paris publication number 2118.

REFERENCES CITED

- Buck, W.R., Lavier, L., and Poliakov, A., 2005, Modes of faulting at mid-ocean ridges: *Nature*, v. 434, p. 719–723.
- Cande, S.C., and Kent, D.V., 1995, Revised calibration of the geomagnetic polarity time scale for the Late Cretaceous and the Cenozoic: *Journal of Geophysical Research*, v. 100, p. 6093–6095.
- Cann, J.R., Blackman, D.K., Smith, D.K., McAllister, E., Janssen, B., Mello, S., Avgerinos, E., Pascoe, A.R., and Escartin, J., 1997, Corrugated slip surfaces formed at North Atlantic ridge-transform intersections: *Nature*, v. 385, p. 329–332.
- Cannat, M., 1996, How thick is the magmatic crust at slow spreading oceanic ridges?: *Journal of Geophysical Research*, v. 101, p. 2847–2857.
- Cannat, M., Lagabrielle, Y., Bougault, H., Casey, J., de Coutures, N., Dmitriev, L., and Fouquet, Y., 1997, Ultramafic and gabbroic exposures at the Mid-Atlantic Ridge: Geological mapping in the 15°N region: *Tectonophysics*, v. 279, p. 193–213.
- Cannat, M., Rommevaux-Jestin, C., Sauter, D., Deplus, C., and Mendel, V., 1999, Formation of the axial relief at the very slow spreading Southwest Indian Ridge (49°–69°E): *Journal of Geophysical Research*, v. 104, p. 22,825–22,843.
- Cannat, M., Rommevaux-Jestin, C., and Fujimoto, H., 2003, Melt supply variations to a magma-poor ultraslow spreading ridge (Southwest Indian Ridge 61° to 69°E): *Geochemistry, Geophysics, Geosystems*, v. 4, 9104, doi: 2002GC000480.
- Dick, H.J.B., Lin, J., and Schouten, H., 2003, An ultraslow-spreading class of ocean ridge: *Nature*, v. 426, p. 405–412.
- Escartin, J., Mével, C., MacLeod, C.J., and McCaig, A.M., 2003, Constraints on deformation conditions and the origin of oceanic detachments: The Mid-Atlantic Ridge core complex at 15°45'N: *Geochemistry, Geophysics, Geosystems*, v. 4, 1067, doi: 2002GC000472.
- Hosford, A., Tivey, M.A., Matsumoto, T., Dick, H.J.B., Schouten, H., and Kinoshita, H., 2003, Crustal magnetization and accretion at the Southwest Indian Ridge near the Atlantis II fracture zone, 0–25 Ma: *Journal of Geophysical Research*, v. 108, 2169, doi: 2001JB000604.
- Jokat, W., Ritzmann, O., Schmidt-Aursch, M.C., Drachev, S., Gauger, S., and Snow, J., 2003, Geophysical evidence for reduced melt production on the Arctic ultraslow Gakkel mid-ocean ridge: *Nature*, v. 423, p. 962–965.
- Klein, E.M., and Langmuir, C.H., 1987, Global corre-

- lations of ocean ridge basalt chemistry with axial depth and crustal chemistry: *Journal of Geophysical Research*, v. 92, p. 8089–8115.
- Kuo, B.Y., and Forsyth, D.W., 1989, Gravity anomalies of the ridge-transform system in the South Atlantic between 31° and 34.5°S: Upwelling centers and variation in crustal thickness: *Marine Geophysical Researches*, v. 10, p. 205–232.
- Lavier, L., Buck, W.R., and Poliakov, A.N.B., 1999, Self-consistent rolling-hinge model for the evolution of large-offset low-angle normal faults: *Geology*, v. 27, p. 1127–1130.
- Lemaux, J., Gordon, R.G., and Royer, J.-Y., 2002, Location of the Nubia-Somalia boundary along the Southwest Indian Ridge: *Geology*, v. 30, p. 339–342.
- Macdonald, K.C., Fox, P.J., Alexander, R.T., Pockalny, R., and Gente, P., 1996, Volcanic growth faults and the origin of Pacific abyssal hills: *Nature*, v. 380, p. 125–129.
- Mendel, V., Sauter, D., Rommevaux-Jestin, C., Patriat, P., and Lefebvre, F., 2003, Magmatotectonic cyclicity at the ultra-slow spreading Southwest Indian Ridge: Evidence from variations of axial volcanic ridge morphology and abyssal hills pattern: *Geochemistry, Geophysics, Geosystems*, v. 4, 9102, doi: 2002GC000417.
- Meyzen, C.M., Toplis, M.J., Humler, E., Ludden, J.N., and Mével, C., 2003, A discontinuity in mantle composition beneath the Southwest Indian Ridge: *Nature*, v. 421, p. 731–733.
- Michael, P.J., Langmuir, C., Dick, H.J.B., Snow, J.E., Goldstein, S.L., Graham, D.W., Lehnert, K., Kurras, G.J., Jokat, W., Mühe, R., and Edmonds, H.N., 2003, Magmatic and amagmatic seafloor generation at the ultraslow-spreading Gakkel ridge, Arctic Ocean: *Nature*, v. 423, p. 956–961.
- Muller, M.R., Minshull, T.A., and White, R.S., 1999, Segmentation and melt supply at the Southwest Indian Ridge: *Geology*, v. 27, p. 867–870.
- Patriat, P., and Segoufin, J., 1988, Reconstruction of the Central Indian Ocean: *Tectonophysics*, v. 155, p. 211–234.
- Reston, T.J., and Ranero, C.R., 2005, Detachment faulting at slow-spreading centres: European Geophysical Union Symposium, Vienna: *Geophysical Research Abstracts*, v. 7, p. 07382.
- Sauter, D., Mendel, V., Rommevaux-Jestin, C., Parson, L.M., Fujimoto, H., Mével, C., Cannat, M., and Tamaki, K., 2004, Focused magmatism versus amagmatic spreading along the ultra-slow spreading Southwest Indian Ridge: Evidence from TOBI side scan sonar imagery.: *Geochemistry, Geophysics, Geosystems*, v. 5, Q10K09, doi: 2004GC000738.
- Searle, R., Cannat, M., Fujioka, K., Mével, C., Fujimoto, H., Bralee, A., and Parson, L., 2003, Fuji Dome: A large detachment fault near 64°E on the very slow-spreading southwest Indian Ridge: *Geochemistry, Geophysics, Geosystems*, v. 4, 9105, doi: 2003GC000519.
- Seyler, M., Cannat, M., and Mével, C., 2003, Evidence for major element heterogeneity in the mantle source of abyssal peridotites from the southwest Indian Ridge (52 to 68° East): *Geochemistry, Geophysics, Geosystems*, v. 4, 9101, doi: 2002GC000305.
- Tucholke, B.E., Lin, J., and Kleinrock, M.C., 1998, Megamullions and mullion structure defining oceanic metamorphic core complexes on the Mid-Atlantic Ridge: *Journal of Geophysical Research*, v. 103, p. 9857–9866.
- Whitmarsh, R.B., Manatschal, G., and Minshull, T.A., 2001, Evolution of magma-poor continental margins from rifting to seafloor spreading: *Nature*, v. 413, p. 150–154.

Manuscript received 21 December 2005

Revised manuscript received 22 February 2006

Manuscript accepted 1 March 2006

Printed in USA